Reaction cross sections for 75–190 MeV alpha particles on targets from ^{12}C to ^{208}Pb

A. Auce,[1] R. F. Carlson,[2] A. J. Cox,[2] A. Ingemarsson,[1,3] R. Johansson,[1] P. U. Renberg,[3] O. Sundberg,[3] G. Tibell,[1] and R. Zorro[3]

[1] *Department of Radiation Sciences, Uppsala University, Uppsala, Sweden*
[2] *University of Redlands, Redlands, California 92373*
[3] *The Svedberg Laboratory, Uppsala, Sweden*

(Received 18 February 1994)

Reaction cross sections for alpha particles have been measured for ^{12}C, ^{16}O, ^{28}Si, ^{40}Ca, ^{48}Ca, ^{58}Ni, ^{60}Ni, ^{124}Sn, and ^{208}Pb at 74.5, 103.2, 129.3, 159.7, and 192.7 MeV. The experimental values are found to be considerably smaller than predictions from conventional optical model calculations.

PACS number(s): 25.55.Ci, 24.10.Ht

I. INTRODUCTION

In elastic scattering experiments the number of experimental data points in the angular distributions is often very large, whereas the reaction cross section, σ_R, consists of just one experimental value. Nevertheless, there is an increasing theoretical interest in reaction cross section data, one reason being that they can be decisive in cases when different models predict similar angular distributions for elastic scattering. Ray [1] has studied proton-nucleus total cross sections in the energy range 100 to 2200 MeV using the nonrelativistic KMT optical model formulation. The calculated reaction cross sections were found to be in good agreement with the experimental results above 400 MeV, but at lower energies these were greater than the experimental results by 15–20%. According to Dymarz [2] this discrepancy is significantly reduced when the scattering is described relativistically, using the Dirac-based impulse approximation optical potential.

Reaction cross sections for different isotopes can also be used for accurate determinations of differences in nuclear matter radii which are essential for information on the differences between proton and neutron distributions in nuclei. This approach was used by Ernst [3] in his analysis of proton reaction cross sections for ^{40,44,48}Ca at 700 MeV and by Dubar *et al.* [4] for the scattering of 96 MeV alpha particles by different isotopes of the nuclei Cr, Fe, Ni, and Sn.

In recent years there has been a great interest in total reaction cross sections for heavy ions. The results have been parametrized in several ways, and have also been extensively used for comparison with predictions of different microscopic models. Recently Hussein, Rego, and Bertulani [5] published a detailed report on the microscopic theory behind different parametrizations.

There are, however, very few results for reaction cross sections for alpha particles. Measurements on several nuclei have been made at Berkeley [6] at 40 MeV and at Kiev at 96–100 MeV [7–11]. Beside these measurements the reaction cross section for ^{12}C was measured at 380 and 620 MeV at Berkeley [12]. Furthermore, Warner *et al.* have reported average reaction cross sections for Si in the energy energy region 27–92 MeV [13] and for ^{127}I and ^{133}Cs in the region 74 to 112 MeV [14].

There were two main goals for the measurements reported here. The first was to increase the reliability of the analyses of a future experiment on the elastic scattering of alpha particles at the The Svedberg Laboratory in Uppsala. The second goal was to gain information about the energy dependence of the reaction cross section for alpha particles in order to make it possible to get a more reliable test of different macroscopic and microscopic models.

II. EXPERIMENTAL EQUIPMENT AND PROCEDURE

At present, the most efficient method to measure reaction cross sections in this energy region is based on the attenuation technique as proposed by Gooding and Eisberg [15] and later modified by Gooding [16] and by Wilkins and Igo [17]. This method has been further improved and successfully used in a number of proton reaction cross section experiments by members of the present group [18], and the same technique is also applied in the alpha particle experiment reported here.

The method used in the present experiment is to measure the attenuation of a beam of particles as it is transmitted through the target. A detailed description of the experimental equipment has been given in Ref. [18].

After passing through the target the incident beam intensity, I_0, has been reduced to I, according to the formula

$$I = I_0 e^{-nx\sigma}, \tag{1}$$

where n is the number of nuclei per unit volume in the target, x the target thickness, and σ the attenuation cross section. If the quantity $nx\sigma$ is small compared to unity, one obtains

$$\sigma = \frac{(I_0 - I)}{nxI_0}. \tag{2}$$

A. Alpha particle beam

A well-collimated alpha particle beam from the Gustaf Werner cyclotron at the The Svedberg Laboratory was directed into our apparatus, shown schematically in Fig. 1. The beam energy spread was approximately 300 keV (FWHM) and the intensity on the target was typically 2×10^4 particles per second.

B. Beam defining counters

The direction and size of the beam at the entrance of the detector system were defined by two collimators, with openings of 1 mm in diameter, placed 3 m apart. By setting discriminator thresholds on the coincident signals from the 0.1 mm thick plastic scintillators 1 and 2, it was possible to identify incident alpha particles. On its way to the target, the beam had to pass through the holes of the detectors 3 and 4, which were in anti-coincidence with counters 1 and 2. In this way particles which had undergone forward scattering in detectors 1 and 2 were eliminated from the trigger.

C. Targets

The targets were mounted on a wheel accommodating 14 targets and an empty space for target-out measurements. They were remotely positioned to an accuracy of 0.1 mm. The details of the different targets are given in Table I. As was the case in a previous proton experiment [19], the oxygen cross section was determined in a comparison between the results using Si and SiO_2 targets.

The ^{48}Ca target was fabricated in 1985. Since then its mass had increased by 7%, due to an accumulated layer of $CaCO_3$. Since reaction cross sections were measured for the contaminants (C and O) in the present experiment, corrections to the measured results for ^{48}Ca were easily made.

D. Energy analyzing telescope

The energy analyzing telescope consisted of detector 5, subtending an angle of $\pm 9°$, and the stopping detector 6, collimated to subtend an angle of $\pm 30°$ as seen from the beam spot on the target. The size of detector 5 and the holes of the annular detectors 3 and 4 were matched to each other in such a way that without the target alpha particles passing through the holes would also go through this detector.

With an acceptance cone half-angle of 30° for detector 6, elastically scattered particles could not escape without depositing all their energy in this detector. All charged particles entering detector 5 were treated electronically as nonreaction events. They constituted more than 98% of the incident flux. The threshold for vetoed events in detector 6 was set at about 10 MeV below the elastic peak energy.

E. Electronic logic

The electronic logic is shown schematically in Fig. 2. The incident beam intensity, I_0, was determined by the signal $12(\overline{3+4})$ and the transmitted, nonreacting beam intensity, I, by $12(\overline{3+4})(5+6)$. A special pile-up rejection circuit prohibited both of two consequtive incident alpha particles from triggering the logic if they arrived within 150 ns of each other. The corrections necessary to determine the reaction cross sections from these raw data are described below.

F. Experimental procedure

An experimental run consisted of data taking periods with the different targets in position, interspaced by target-out measurements at frequent intervals. The uncorrected reaction cross section is determined from the difference between the terms $(I_0 - I)$ and the corresponding quantity $(i_0 - i)$ obtained from target-out measurements.

G. Corrections to the raw data

The uncorrected reaction cross section $\sigma_{\rm un}$ was obtained from

$$\sigma_{\rm un} = \frac{1}{nx}\left[\frac{(I_0 - I)}{I_0} - \frac{(i_0 - i)}{i_0}\right]. \quad (3)$$

In the following the corrections applied to the raw data are described. They are mostly small and of different signs, so that in the end they almost cancel.

(i) The first correction concerned elastically scattered alpha particles which emerged at angles greater than 30° and thus missed detector 6. These nonreaction events were falsely counted as reactions since there was no gate-

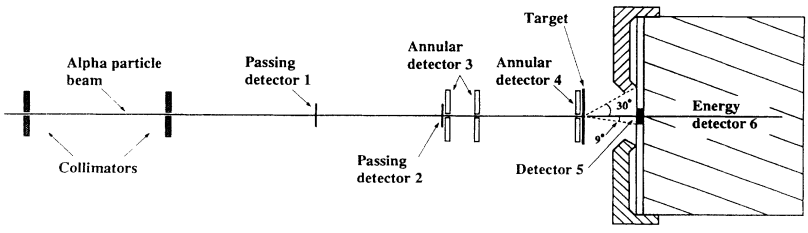

FIG. 1. Schematic diagram of the total reaction cross section apparatus.

TABLE I. Target specifications.

Target	Enrichment	Thickness (mg/cm^2)	Thickness nonuniformity %
^{12}C	Natural	78.9	0.5
SiO_2	Natural	62.0	0.1
^{28}Si	Natural	77.4	0.1
^{40}Ca	Natural	49.0	4
^{48}Ca	90.8%	10.9	2
^{58}Ni	99.79%	40.5	2
^{60}Ni	99.07%	39.5	2
^{124}Sn	96.71	38.5	2
^{208}Pb	99.86	67.4	4

closing signal from either detector 5 or 6. The experimentally measured σ_{un} was corrected by subtracting the elastic differential cross section integrated between 30° and 180°. These elastic cross sections were taken from published data [20–45]. The correction subtracted was always less than 2% of σ_{un}.

(ii) The second correction was for nuclear reactions producing charged particles which missed detector 5, but entered detector 6 ($9° < \theta < 30°$) with energies above the discriminator level for that detector. These were thus falsely counted as elastic events. A correction was applied for these missing reaction events. In most cases the discriminator level for detector 6 was set 10 MeV (ΔE) below the elastic peak. The appropriate cross sections (Refs. [33,34,38,40–42,44–48]) were integrated to give the charged particle reaction correction,

$$2\pi \int_{9°}^{30°} \sin\theta \, d\theta \int_{E-\Delta E}^{E} \frac{d\sigma}{dE \, d\Omega} dE. \quad (4)$$

This positive correction was always less than 2.5% of σ_{un}.

(iii) Reaction products which triggered detector 5 were registered as nonreaction events. This correction was in general quite small, since the solid angle subtended by detector 5 from the target was only 0.077 sr. It was measured using a method suggested by an Oak Ridge group [49]. The correction added was typically less than 0.6%.

(iv) Some alpha particles were elastically scattered outside detector 5 but into detector 6 and then lost energy through nuclear reactions in the detector material, thus producing false reaction events. As mentioned above, detector 5 significantly reduced the number of such events. In order to estimate this correction a separate experiment was performed to measure the reaction rate for alpha particles in detector 6 using the same technique reported in Ref. [50] for protons. The correction was negative and less than 1%.

(v) Effects such as finite target thickness and finite beam size did not contribute significantly to the experimental error.

III. EXPERIMENTAL RESULTS

The reaction cross sections obtained at the five energies are presented in Table II. The quoted errors are statistical. The beam energies were determined with a time-of-flight technique with uncertainties less than 0.5 MeV.

The results are shown in Fig. 3 by the solid circles. Proton reaction cross sections are shown by the open circles at the same energy per nucleon. Besides data taken from the compilation of Bauhoff [51] results for ^{48}Ca [52], and unpublished results for ^{58}Ni and ^{60}Ni [53], and ^{124}Sn [54] are shown. As expected the values are considerably larger for alpha particles than for protons. It is somewhat surprising, however, that the energy dependence is so different in the two cases. For ^{12}C the reaction cross sections for protons are almost constant whereas the values for alpha particles decrease with energy. For ^{208}Pb the values for alpha particles stay almost constant, whereas the values for protons increase with energy. Optical model calculations have shown that the increase in the proton reaction cross sections for heavy nuclei may be well understood as a Coulomb effect [19,55]. This energy dependence is represented by Eq. (5) (in the next section) in which the Coulomb barrier acts to inhibit the reaction cross section at lower energies for heavy nuclei such as ^{208}Pb. Since the slope due to the Coulomb interaction is proportional to the charge product and inversely proportional to the incident energy, the slope for the reaction cross sections for alpha particles should be half as large as for protons if it was a pure Coulomb effect. Apparently this is not the case.

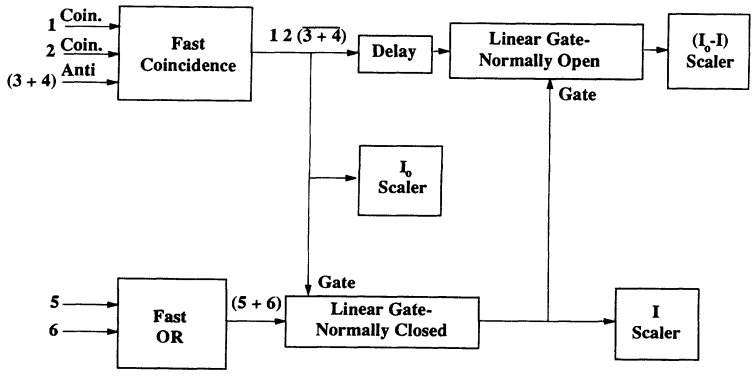

FIG. 2. Schematic diagram of the electronic logic.

TABLE II. Experimental results for the reaction cross sections (mb) for alpha particles.

Target	Incident energy (MeV)				
	74.5	103.2	129.3	159.7	192.7
^{12}C	848±14	745±20	685±15	597±11	544±14
^{16}O	945±10	849±17	809±15	718±11	663±21
^{28}Si	1161±14	1083±14	1042±17	938±15	885±20
^{40}Ca	1361±24	1280±20	1262±20	1093±32	1039±33
^{48}Ca	1626±65	1421±47	1393±46	1341±47	1282±34
^{58}Ni	1511±21	1468±25	1465±15	1381±46	1329±14
^{60}Ni	1551±16	1459±21	1523±30	1429±45	1384±14
^{124}Sn	2127±30	2084±30	2182±36	1971±52	2016±40
^{208}Pb	2653±85	2574±48		2545±75	2476±52

IV. PARAMETRIZATION OF THE EXPERIMENTAL RESULTS

The reaction cross section is a measure of the probability that an incident particle will undergo an inelastic reaction anywhere in the nucleus, and it is therefore natural to asume that it is closely related to the size and shape of the nucleus. In Ref. [56] calculations using the Glauber approximation showed that the reaction cross section is proportional to the number of nucleons, A or R^3, when the nucleon-nucleon interaction is very weak. When the strength increases, the dependence on R becomes weaker, and when the total cross section is just below 40 mb the calculated reaction cross section was found to be proportional to $A^{2/3}$ or R^2. The isospin average value of the nucleon-nucleon interaction varies smoothly around this value in the energy region 200–1000 MeV. This explains why it was possible in a previous experiment to parametrize [57] the reaction cross section for protons in the energy range 200–800 MeV with the formula

$$\sigma_R = \pi \left(r_0 A^{1/3} + \lambda\right)^2 \left[1 - \frac{Zze^2}{(R+\lambda)E_0}\right][1-T]. \quad (5)$$

In this equation, r_0 is the effective reduced nuclear radius, λ the reduced wavelength of the incident particle, z and Z the charge of the incident particle and the target nucleus, respectively, and T is the transparency which may be related to the mean free path of the projectile in nuclear matter. It should be mentioned that such a parametrization was suggested by Bethe as early as 1940 [58].

The successful parametrizations for protons have implied that the dependence on R^2 be used also for other more strongly interacting particles. There is a wide variety of parametrizations which take into account different effects. The microscopic theory behind these was recently discussed by Hussein, Rego, and Bertulani [5].

As mentioned above, experimental results for the reaction cross sections for alpha particles for several nuclei are

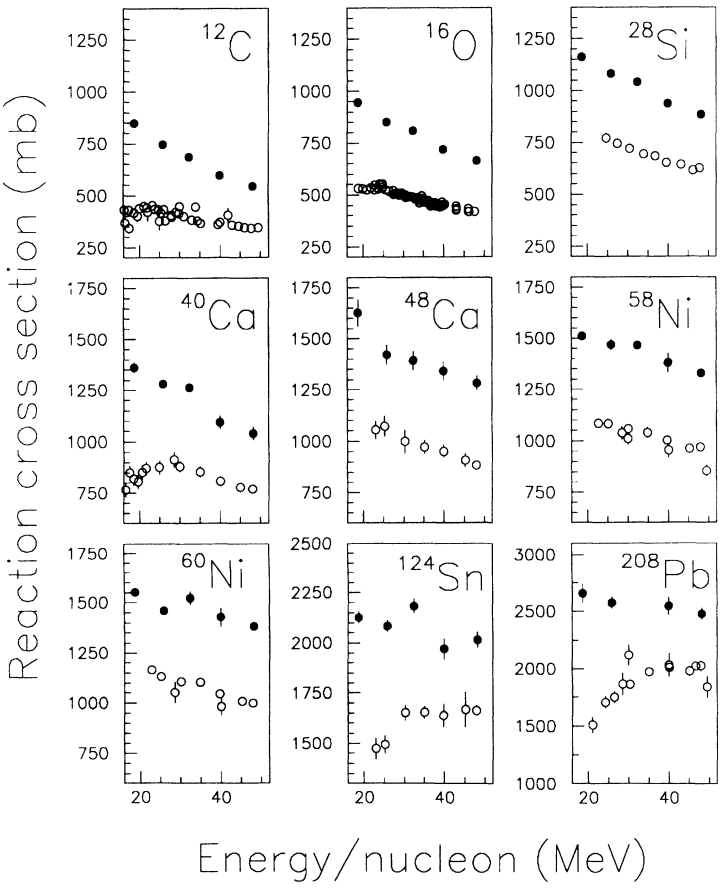

FIG. 3. Experimental values of the reaction cross section for alpha particles (solid circles) and for protons (open circles) versus energy per nucleon. The results for protons are from the compilation of Bauhoff [51] and Refs. [52–54].

only available at 40 MeV and 100 MeV. Recently Dubar *et al.* [11] parametrized the 100 MeV data successfully with the expression

$$\sigma_R = \pi(R_A A_T^{1/3} + 1.12 A_\alpha^{1/3})^2, \quad (6)$$

where A_T and A_α are the mass numbers of the target and the incident alpha particle, respectively. They found that this parametrization, with $R_A = 1.30$, was more successful than sophisticated expressions with Coulomb and other corrections. Such a parametrization also worked well for protons at 60.8 and 100 MeV, for ^{12}C at 30, 83, 200, and 300 MeV per nucleon, for ^{16}O at 30 MeV per nucleon, and for ^{20}Ne at 100 and 300 MeV per nucleon.

We compare our results at 103.2 MeV with the 100 MeV data from Kiev in Fig. 4. The reaction cross sections are plotted versus $(A_T^{1/3}+A_\alpha^{1/3})^2$. One observes that the two experiments are in fair agreement, and that there is an almost linear relation between the reaction cross sections and $(A_T^{1/3} + A_\alpha^{1/3})^2$. The two experiments are also in good agreement with the energy averaged value for Si, 1170±55 mb, obtained by Warner *et al.* [13] in the energy region 27–92 MeV. The dashed line shows the parametrization according to Eq. (6) which deviates smoothly from a straight line. The solid line shows the parametrization with the usual heavy-ion relation between the reduced and the effective radius, given by

$$\sigma_R = \pi r_0^2 (A_T^{1/3} + A_\alpha^{1/3})^2. \quad (7)$$

This parametrization was found to give essentially the same χ^2 value as Eq. (6) for our data at 103.2 MeV.

The A_T dependence at the other energies is rather similar as shown in Fig. 5. In general, for all energies and values of A_T, the reaction cross sections, divided by $(A_T^{1/3} + A_\alpha^{1/3})^2$ are rather constant. However, for light nuclei one observes a deviation from this trend. At 74.5 MeV these values are slightly higher while they are lower for the three highest energies. In an attempt to take this effect into account we also parametrized the data with two parameters according to

$$\sigma_R = \pi(r_A A_T^{1/3} + r_\alpha A_\alpha^{1/3})^2. \quad (8)$$

The solid curves in Fig. 5 show the parametrization according to Eq. (8) and the dashed lines according to Eq. (7). The values of the parameters are given in Table III.

It is surprising that it is possible to reproduce the reaction cross section data so well with only one or two free parameters at each energy. As discussed in Ref. [59] the real potential for alpha particles in this energy region is so strong that it has a considerable effect on the imaginary phase shifts and the absorption. It was mentioned above that Coulomb corrections to the parametrization do not give better agreement with the experimental data. This fact indicates that there is a cancellation between the corrections due to the real and the Coulomb potentials. This

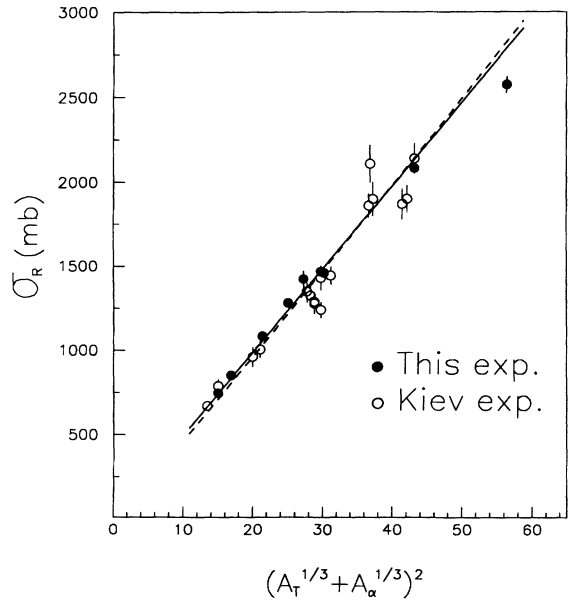

FIG. 4. Reaction cross sections obtained at 103.2 MeV in this experiment and at 100 MeV in Kiev plotted versus $(A_T^{1/3} + A_\alpha^{1/3})^2$.

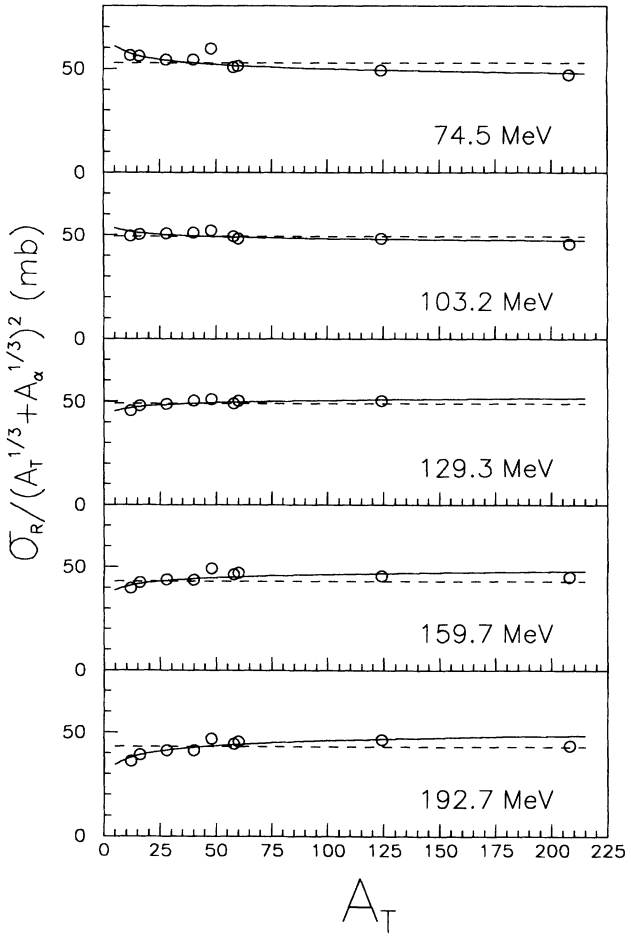

FIG. 5. Experimental reaction cross sections divided by $(A_T^{1/3} + A_\alpha^{1/3})^2$ plotted versus the atomic number A_T. The dashed and solid curves show the parametrizations with Eq. (7) and Eq. (8), respectively.

TABLE III. Best fit parameter values obtained with the reaction cross sections parametrized according to Eqs. (7) and (8).

E (MeV)	Eq. (7)		Eq. (8)		
	r_0 (fm)	χ^2	r_A (fm)	r_α (fm)	χ^2
74.5	1.296	119.4	1.112	1.693	15.1
103.2	1.251	36.4	1.159	1.464	14.9
129.3	1.251	22.4	1.344	1.047	7.4
159.7	1.175	53.8	1.321	0.895	20.2
192.7	1.183	125.5	1.371	0.739	47.2

is supported by the results for the scattering of 140 MeV alpha particles in Ref. [60], where exact optical model calculations with and without the Coulomb interaction give a difference of 8%, or 125 mb. The Glauber calculations, however, without any noneikonal corrections, deviate only 27 mb from the optical model value.

V. DISCUSSION OF THE RESULTS FOR ^{12}C

In the case of ^{12}C there exist a few measurements at energies higher than those studied here. There is thus a possibility to investigate the energy dependence of reaction cross sections over an extended energy region. Figure 6 presents experimental reaction cross section data for alpha particles, protons, deuterons, and ^{12}C ions. The horizontal axis denotes energy per nucleon on a logarithmic scale. Our results are shown as solid circles. The solid triangles show the experimental results for alpha particles at 40 [6], 100 [8], 348, and 648 MeV [12]. We have also included the result from a measurement of the alpha particle absorption cross section at 3480 MeV [61], since it should be very similar to the reaction cross section at this energy [61]. The open circles show the results for protons, the open triangles represent two results for deuterons [62,63] and the stars the results for ^{12}C ions [64,65]. The solid curves show the p-p and n-p total cross sections and their sum. We observe that whereas the reaction cross sections for alpha particles over this region are much greater than those for protons, they are essentialy the same as those for deuterons but considerably smaller than those for ^{12}C.

DeVries and Peng [66] have discussed the relation between the nucleus-nucleus reaction cross sections and the total cross section for the nucleon-nucleon system. We observe in Fig. 6 that the energy dependences of the reaction cross sections for alpha particles and ^{12}C ions are very similar with a falloff up to about 100 MeV per nucleon followed by a smooth leveling off. The same behavior is characteristic also for the nucleon-nucleon total cross section as seen in Fig. 6. It should be remarked, however, that the falloff for low energies becomes less pronounced for heavier nuclei as shown in Fig. 3. It is quite natural, however, that the geometrical effects have a larger effect than the nucleon-nucleon interaction for heavier nuclei. The fact that the reaction cross sections

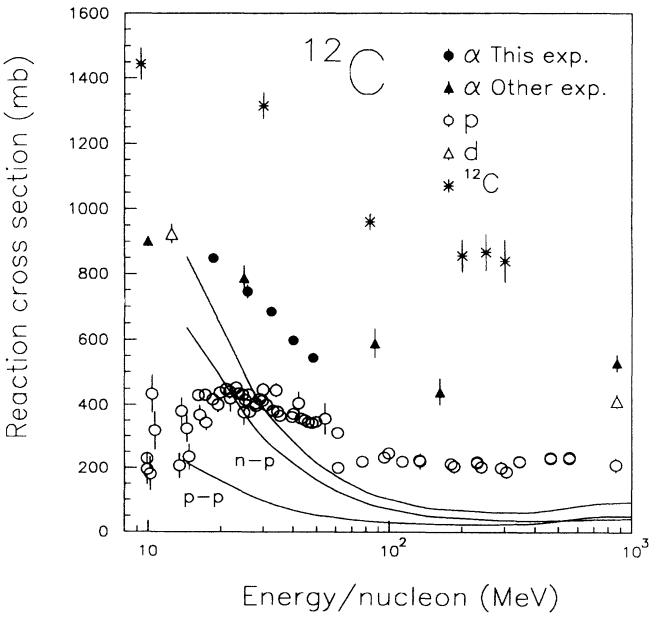

FIG. 6. Experimental reaction cross sections for ^{12}C obtained with alpha particles, protons, deuterons, and ^{12}C ions. The solid lines show the p-p and n-p total cross sections and the sum of these.

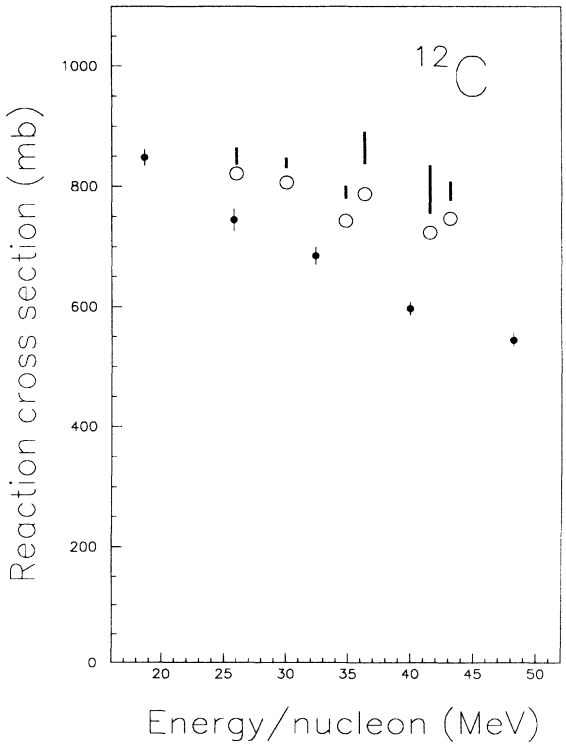

FIG. 7. Reaction cross sections for ^{12}C. The open circles show the results obtained from optical model calculations performed with a Woods-Saxon parametrization. The vertical lines show the results from the folding model calculations in Ref. [67].

have about the same magnitude for deuterons and alpha particles, in spite of the fact that the radius of the deuteron is larger than the radius of the alpha particle, indicates that the geometrical effects and the strength of the fundamental interaction are both very important in the case of ^{12}C.

VI. OPTICAL MODEL CALCULATIONS

We calculated the reaction cross sections in the optical model using a conventional Woods-Saxon parametrization of the potential. Figure 7 shows the results obtained for ^{12}C. The potentials were obtained from a fitting procedure to Karlsruhe data at 104 MeV [29], Jülich data at 120, 145, and 172.5 MeV [35–37], Maryland data at 139 MeV [42], and Orsay data at 166 MeV [34]. The calculated values are shown as open circles, and our experimental data as solid circles. As can be seen the calculations overestimate the reaction cross sections, and the difference seems to increase with energy. At 172.5 MeV, where the elastic scattering data are quite accurate, the interpolated experimental value is 577 mb whereas the optical model value is 747 mb. It turned out that it was impossible to reproduce simultaneously the elastic angular distribution and the reaction cross section with the Woods-Saxon parametrization of the optical potential. When a new search, constrained to reproduce the reaction cross section was performed, the diffraction pattern in the angular distribution at small angles was shifted in an unacceptable way.

Most optical model codes do not take into account the effects of relativistic kinematics on the Rutherford cross section [60]. Since this quantity is often used in the absolute normalization of the differential cross sections, we decided to investigate to what extent a renormalization of the experimental angular distributions affected the reaction cross section. It turned out, however, that even with a renormalization of 10%, the reaction cross section varied less than 5%. This indicates that a simultaneous reproduction of the elastic angular distribution and the reaction cross section requires a more sophisticated optical potential.

In Ref. [67] some of the present authors analyzed the elastic scattering by several nuclei using a simple single-folding model for the real and imaginary potentials. For different values of the range of the real folding parameter β_r, the imaginary folding parameter β_i, the radius and the diffuseness of the matter distribution, and the strengths of the Gaussian interactions were determined to give a best fit to the angular distributions. The resulting angular distributions were found to be very similar for

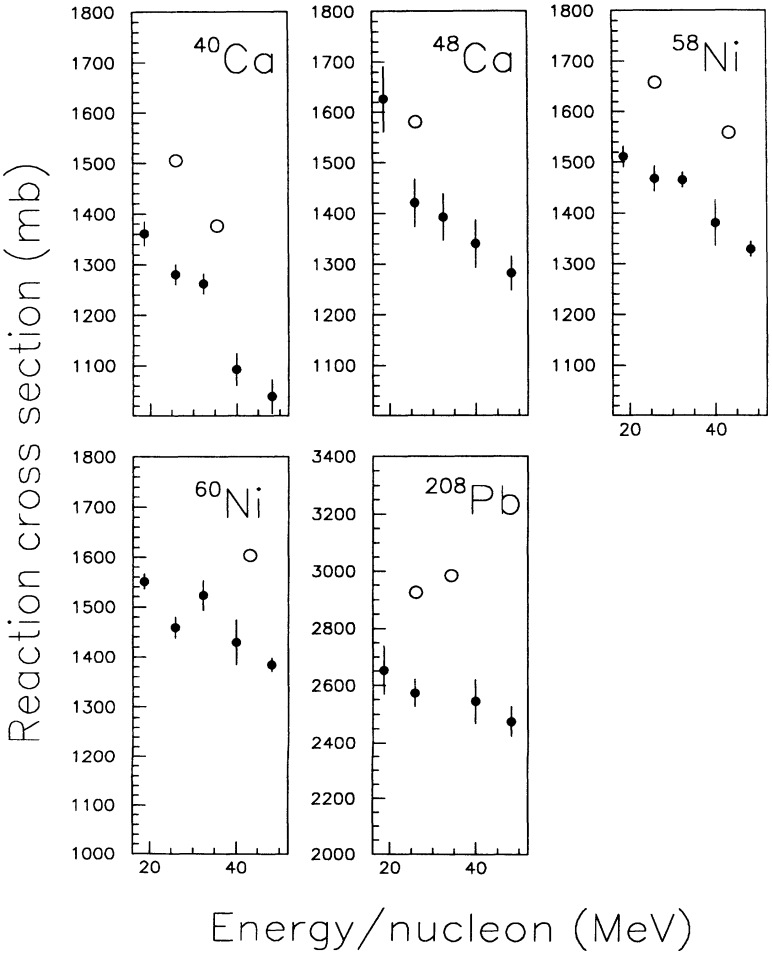

FIG. 8. Experimental reaction cross sections for alpha particles and values (open circles) calculated in optical model calculations using Woods-Saxon potentials.

different values of β_r. The variation in the reaction cross sections for values of β_r between 1 fm and 2 fm is shown by the vertical lines in Fig. 7. The fact that these values vary with β_r and differ from those obtained with Woods-Saxon potentials show that the reaction cross section is sensitive to the shape of the potentials.

In Ref. [12] DeVries *et al.* compare the energy dependence of the reaction cross section for alpha particles on ^{12}C with a calculation in the Glauber approximation. Their curve is in good agreement with the experimental results. This is due to the fact that they did not take into account the noneikonal effects due to the real potential, which are very large. In our optical model calculations, the reaction cross section was reduced by 125 mb at 104 MeV and by 70 mb at 172.5 MeV when the real potential was omitted in the calculations.

Also for the other nuclei the optical model calculations with Woods-Saxon potentials overestimate the reaction cross sections. This is illustrated in Fig. 8. In all cases the difference is at least 10%. In the case of ^{58}Ni the calculations in Ref. [65] were performed with both the real and imaginary potentials folded (ff-case) as well as with the real potential folded and the imaginary potential of the Woods-Saxon shape (fws-case). It turned out that the reaction cross section varied much more in the fws-case than in the ff-case. For values of β_r between 1 fm and 2 fm the reaction cross section varied between 1671 and 1686 mb in the ff-case and between 1584 and 1680 mb in the fws-case.

All these results indicate that the reaction cross section is very sensitive to the shapes of the optical potentials. The fact that our models strongly overestimate the reaction cross sections may be taken as an indication that more sophisticated potential models need to be used to reproduce simultaneously angular distributions and reaction cross sections.

VII. CONCLUSIONS

The reported reaction cross-section data for intermediate energy alpha particles could be very well parametrized with one single parameter. We believe that the effects from the attractive nuclear potential to a large extent cancel the effects from the repulsive Coulomb potential.

The values of the experimental reaction cross sections are considerably smaller than values calculated from the simple optical models we have used. We have shown that reaction cross sections are sensitive to the shape of the potentials, but more sophisticated calculations are required to obtain a detailed knowledge of them. Thus, the data should be studied with potentials obtained by double-folding including density dependence and other effects. The data also offer an interesting possibility to compare the nonrelativistic and relativistic approaches. The fact that the simple models fail so drastically makes us believe that our data will play a decisive role in future analyses of scattering of intermediate energy alpha particles.

ACKNOWLEDGMENTS

We want to thank W. T. H. van Oers for initiating the contacts between the groups in Uppsala and Redlands and Robert Peterson for his work on our vacuum system. The work at the University of Redlands was supported by the Research Corporation.

[1] L. Ray, Phys. Rev. C **20**, 1857 (1979).
[2] R. Dymarz, Phys. Lett. **152B**, 319 (1985).
[3] D. J. Ernst, Phys. Rev. C **19**, 896 (1979).
[4] L. V. Dubar, D. Sh. Eleunokov, O. F. Nemets, L. I. Slyusarenko, V. V. Tokarevsky, and N. P. Yurkuts, Bull. Acad. Sci. USSR, Phys. Ser. **56**, 453 (1992).
[5] M. S. Hussein, R. A. Rego, and C. A. Bertulani, Phys. Rep. **201**(5), 279 (1991).
[6] G. Igo and B. D. Wilkins, Phys. Rev. **131**, 1251 (1963).
[7] L. N. Gorovenko, V. N. Domnikov, L. V. Dubar, V. S. Zaritskii, D. Sh. Eleukenov, O. F. Nemets, V. V. Skorohod, L. I. Slyusarenko, S. M. Solonin, V. V. Tokarevskii, and N. P. Yurkuts, Bull. Acad. Sci. USSR, Phys. Ser. **52**, 82 (1988).
[8] V. N. Domnikov, L. V. Dubar, V. A. Zybin, D. Sh. Eleukenov, O. F. Nemets, L. I. Slyusarenko, V. V. Tokarevskii, and N. P. Yurkuts, Bull. Acad. Sci. USSR, Phys. Ser. **52**, 62 (1988).
[9] V. P. Badovskij, L. N. Gorovenko, L. V. Dubar, V. A. Zybin, D. Sh. Eleukenov, O. F. Nemets, L. I. Slyusarenko, V. A. Stepanenko, V. V. Tokarevskii, and N. P. Yurkuts, Bull. Acad. Sci. USSR, Phys. Ser. **51**, 185 (1987).
[10] V. S. Bulkin, V. N. Domnikov, L. V. Dubar, V. A. Zybin, D. Sh. Eleukenov, O. F. Nemets, L. I. Slyusarenko, V. V. Tokarevskii, and N. P. Yurkuts, Yad. Fiz. **43**, 1368 (1986) [Sov. J. Nucl. Phys. **43**, 880 (1986)].
[11] L. V. Dubar, D. Sh. Eleukenov, L. I. Slyusarenko, N. P. Yurkuts, Yad. Fiz. **49**, 1239 (1989) [Sov. J. Nucl. Phys. **49**, 771 (1989)].
[12] R. M. DeVries, N. J. DiGiacomo, J. S. Kapustinsky, J. C. Peng, W. E. Sondheim, J. W. Sunier, J. G. Cramer, R. E. Loveman, C. R. Gruhn, and H. H. Wieman, Phys. Rev. C **26**, 301 (1982).
[13] R. E. Warner, A. M. Van den Berg, K. M. Berland, J. D. Hinnefled, Z. Zhang, Y. T. Zhu, X. Q. Hu, and S. Li, Phys. Rev. C **40**, 2473 (1989).
[14] R. E. Warner, H. W. Wilschut, W. F. Rulla, and G. N. Felder, Phys. Rev. C **43**, 1313 (1991).
[15] T. J. Gooding and R. M. Eisberg, Annual Report, University of Minnesota, 1957–1958 (unpublished), p. 57.
[16] T. J. Gooding, Nucl. Phys. **12**, 214 (1959).
[17] B. D. Wilkins and G. J. Igo, Phys. Rev. **129**, 2198 (1963).
[18] R. F. Carlson, W. F. McGill, T. H. Short, J. M. Cameron, J. R. Richardson, W. T. H. van Oers, J. W. Verba, P. Doherty, and D. J. Margaziotis, Nucl. Instrum. Methods **123**, 509 (1975).

[19] R. F. Carlson, A. J. Cox, J. R. Nimmo, N. E. Davison, S. A. Elbakr, J. L. Horton, A. Houdayer, A. M. Sourkes, W. T. H. van Oers, and D. J. Margaziotis, Phys. Rev. C **12**, 1167 (1975).
[20] H. J. Gils, E. Friedman, H. Rebel, J. Buschmann, S. Zagromski, H. Klewe-Nebenius, B. Neumann, R. Pesl, and G. Bechtold, Phys. Rev. C **21**, 1239 (1980).
[21] H. J. Gils, E. Friedman, H. Rebel, J. Buschmann, S. Zagromski, H. Klewe-Nebenius, B. Neuman, R. Pesl, and G. Bechtold, Report No. KfK-2838, Kernforschungszentrum, Karlsruhe.
[22] H. J. Gils, Report No. KfK-3765, Kernforschungszentrum, Karlsruhe.
[23] H. J. Gils, H. Rebel, and E. Friedman, Report No. KfK-3556, Kernforschungszentrum, Karlsruhe.
[24] H. J. Gils, H. Rebel, and E. Friedman, Phys. Rev. C **29**, 1295 (1984).
[25] H. J. Gils, Report No. KfK-2225, Kernforschungszentrum, Karlsruhe.
[26] H. J. Gils, E. Friedman, Z. Majka, and H. Rebel, Phys. Rev. C **21**, 1245 (1980).
[27] H. J. Gils and H. Rebel, Z. Phys. A **274**, 259 (1975).
[28] H. J. Gils, H. Rebel, J. Buschmann, H. Klewe-Nebenius, G. P. Nowicki, and W. Nowatzke, Z. Phys. A **279**, 55 (1976).
[29] G. Schatz, G. W. Schweimer, and J. Specht, Nucl. Phys. **A128**, 81 (1969).
[30] V. Corcalciuc, H. Rebel, R. Pesl, and H. J. Gils, J. Phys. G: Nucl. Phys. **9**, 177 (1983).
[31] D. A. Goldberg, S. M. Smith, and G. F. Burdzik, Phys. Rev. C **10**, 1362 (1974).
[32] P. L. Roberson, D. A. Goldberg, N. S. Wall, L. W. Woo, and H. L. Chen, Phys. Rev. Lett. **42**, 54 (1979).
[33] D. A. Goldberg, S. M. Smith, H. G. Pugh, P. G. Roos, and N. S. Wall, Phys. Rev. C **7**, 1938 (1973).
[34] B. Tatischeff and I. Brissaud, Nucl. Phys **A155**, 89 (1970).
[35] S. Wiktor, C. Mayerbor, A. Kiss, M. Rogge, P. Turek, and H. Dabrowski, Acta Phys. Pol. B **12**, 491 (1981).
[36] J. Albinski, A. Budzanowski, H. Dabrowski, Z. Rogalska, and S. Wiktor, Nucl. Phys. **A445**, 477 (1985).
[37] A. Kiss, C. Mayerbor, M. Rogge, P. Turek, and S. Wiktor, J. Phys. G **13**, 1067 (1987).
[38] H. Eickhoff, D. Frekers, H. Löhner, K. Poppensieker, G. Gaul, C. Mayer-Böricke, and P. Turek, Nucl. Phys. **A252**, 333 (1975).
[39] F. Michel, J. Albinski, P. Belery, Th. Delbar, Gh. Gregoire, B. Tasiaux, and G. Reidemeister, Phys. Rev. C **28**, 1904 (1983).
[40] K. T. Knöpfle, G. J. Wagner, H. Breuer, M. Rogge, and C. Mayer-Böricke, Phys. Rev. Lett. **35**, 779 (1975).
[41] I. Brissaud, B. Tatischeff, L. Bimbot, V. Comparat, A. Willis, and M. K. Brussel, Phys. Rev. C **6**, 595 (1972).
[42] S. M. Smith, G. Tibell, A. A. Cowley, D. A. Goldberg, H. G. Pugh, W. Reichart, and N. S. Wall, Nucl. Phys. **A207**, 273 (1973).
[43] H. Rebel, G. W. Schweimer, G. Schatz, J. Specht, R. Löhken, G. Hauser, D. Habs, and H. Klewe-Nebenius, Nucl. Phys. **A182**, 145 (1972).
[44] M. N. Harakeh, A. R. Arends, M. J. de Voigt, A. G. Drentje, S. Y. van der Werf, and A. van der Woude, Nucl. Phys. **A265**, 189 (1976).
[45] H. Rebel, G. W. Schweimer, G. Schatz, J. Specht, R. Löhken, G. Hauser, D. Habs, and H Klewe-Nebenius, Phys. Rev. Lett. **26**, 1190 (1971).
[46] J. Specht, H. Rebel, G. Schatz, G. W. Schweimer, G. Hauser, and R. Löhken, Nucl. Phys. **A143**, 373 (1970).
[47] L. Bimbot, I. Brissaud, B. Tatischeff, Y. Le Bornec, N. Frascaria, and A. Willis, Nucl. Phys. **A210**, 397 (1973).
[48] K. T. Knöpfle, G. J. Wagner, A. Kiss, M. Rogge, C. Mayer-Böricke, and Th. Bauer, Phys. Lett. **64B**, 263 (1976).
[49] J. J. H. Menet, E. E. Gross, J. J. Malanify, and A. Zucker, Phys. Rev. C **4**, 1114 (1971).
[50] For example, see A. M. Sourkes, M. S. de Jong, C. A. Goulding, W. T. H. van Oers, E. A. Ginkel, R. F. Carlson, A. J. Cox, and D. J. Margaziotis, Nucl. Instrum. Methods **143**, 589 (1977).
[51] W. Bauhoff, At. Data Nucl. Data Tables **35**, 425 (1986).
[52] R. F. Carlson, A. J. Cox, N. E. Davison, T. Eliyakut-Roshko, R. H. McCamis, and W. T. H. van Oers, Phys. Rev. C **49**, 3090 (1994).
[53] T. Eliyakut-Roshko, R. H. McCamis, W. T. H. van Oers, R. F. Carlson, and A. J. Cox, submitted to Phys. Rev. C.
[54] R. F. Carlson, private communication.
[55] R. Abegg, J. Birchall, N. E. Davison, M. S. de Jong, D. L. Ginther, D. K. Hasell, T. N. Nasr, W. T. H. vanOers, R. F. Carlson, and A. J. Cox, Nucl. Phys. **A324**, 109 (1979).
[56] G. Fäldt and A. Ingemarsson, Phys. Scr. **28**, 136 (1983).
[57] P. U. Renberg, D. F. Measday, M. Pepin, P. Schwaller, B. Favier, and C. Richard-Serre, Nucl. Phys. **A193**, 81 (1972).
[58] H. A. Bethe, Phys. Rev. **57**, 1125 (1940).
[59] A. Ingemarsson and G. Fäldt, Phys. Rev. C **48**, 507 (1993).
[60] G. Fäldt, A. Ingemarsson, and J. Mahalanabis, Phys. Rev. C **46**, 1974 (1992).
[61] J. Jaros, A. Wagner, L. Anderson, O. Chamberlain, R. Z. Fuzesy, J. Gallup, W. Gorn, L. Schroeder, S. Shannon, G. Shapiro, and H. Steiner, Phys. Rev. C **18**, 2273 (1978).
[62] S. Mayo, W. Schimmerling, R. M. Sametband, and R. M. Eisberg, Nucl. Phys. **22**, 393 (1965).
[63] J. D. Jafar, T. J. MacMahon, H. B. von der Raay, D. H. Reading, K. Ruddick, and D. G. Ryan, Nuovo Cimento **48**, 1437 (1967).
[64] C. Perrin, S. Kox, N. Longequeue, J. B. Viano, M. Buenerd, R. Cherkaoui, A. J. Cole, A. Gamp. J. Menet, R. Ost, R. Bertholet, C. Guet, and J. Pinston, Phys. Rev. Lett. **49**, 1905 (1982).
[65] S. Kox, A. Gamp, C. Perrin, J. Arvieux, R. Bertholet, J. F. Bruandet, M. Buenerd, Y. El Masri, N. Longequeue, and F. Merchez, Phys. Lett. **159B**, 15 (1985).
[66] R. M. DeVries and J. C. Peng, Phys. Rev. C **22**, 1055 (1980).
[67] A. Ingemarsson, A. Auce, and R. Johansson, Phys. Rev. C **49**, 1609 (1994).